-RESEARCH PAPER-

International Journal of Mining and Geo-Engineering

IJMGE

IJMGE 58-3 (2024) 307-313

DOI: 10.22059/IJMGE.2024.369958.595133

Evaluation of effective geomechanical parameters in rock mass cavability using different intelligent techniques

Behnam Alipenhani [a], Hassan Bakhshandeh Amnieh [a, *], Abbas Majdi [a]

[a] *School of Mining Engineering, College of Engineering, University of Tehran, Tehran, Iran.*

Article History:

Received: 21 December 2023.
Revised: 22 May 2024.
Accepted: 14 July 2024.

ABSTRACT

The paper presents the results of a comprehensive investigation of the applicability of various intelligence methods for the optimal prediction of rock mass caveability in block caving using effective geomechanical parameters. However, due to the complexity of the prediction of rock mass cavability, artificial intelligence-based methods, including the classification and regression tree (CART), support vector machines (SVM), and artificial neural network (ANN), have been selected. For validating and comparing the results, common MVR was used. Because of the dependency of the modelling generality and accuracy on the number of data, we attempted to obtain an adequate database from the results of numerical modelling. The distinct element method (DEM) used to study the rock mass cavability. The results indicated that ANN is the most accurate modelling technique with a determination coefficient of 0.987 compared with the other aforesaid methods. Finally, the sensitivity analysis showed that joint spacing, friction angle, joint set number, and undercut depth are the most prevailing parameters of rock mass cavability. However, the joint dip has shown the minimum effect on rock mass cavability in the block caving mining method.

Keywords: *Block caving, Cavability, Jointed rock mass, Numerical modelling, Artificial intelligence techniques..*

1. Introduction

Estimating rock mass cavability is an essential variable in block, panel, and mass caving methods. However, inadequate estimation of this variable can result in the loss of all or part of the ore body. Determining the minimum span at which caving initiates and propagates directly affects the rock mass cavability. The minimum required caving span is a function of controllable parameters (draw rate, undercut geometry, etc.) and uncontrollable parameters (geomechanical rock mass properties).

Various methods were employed to assess the rock mass cavability, including numerical methods [1-7] that analyze the ability to initiate and propagate caving. Empirical methods [8-11] based on the data from block caving mines and open stopes establish a relationship between the hydraulic radius of caving and MRMR, Q and DRMR classification systems. These methods provided diagrams to determine the hydraulic radius and minimum caving span. Probabilistic methods [12-15] determine the cavability index based on scoring the impact of various parameters. The lack of a statistical relation for choosing the minimum required caving span is this issue investigated in this paper. All these methods have been used for this purpose.

Artificial Intelligence (AI) is used in various mining and geological engineering projects, which is a helpful method for coping with these problems [16-21].

Most recent studies have focused on the evaluation of cavability. The history of cavability evaluation methods is fully mentioned by Alipenhani *et al* [11]. Rafiee [14] used a rock engineering system (RES), which analyses the interrelationships between the effective parameters to study the cavability of rock. He also used a fuzzy system to minimize the subjectivity of weights calculated in the RES method. Suzuki et al. investigated parameters affecting cave mining using numerical modelling [6]. Jabinpour et al. investigated rock mass cavability using geostatistical modelling based on the laubscher approach in Sechahoon Mine [15].

Mohamadi et al. [12] have presented a hybrid probabilistically qualitative–quantitative model to evaluate the cavability of immediate roof and to estimate the main caving span in longwall mining by combining the empirical model and the numerical solution. For this purpose, numerical simulation was incorporated into the Roof Strata Cavability index (RSCi) as a summation of ratings for nine significant parameters. A distinct element code was used to simulate numerically the main caving span corresponding to various RSCi classes probabilistically.

Alipenhani et al. [4] present the results of a comprehensive investigation into the applicability of various intelligence methods for the optimal prediction of rock mass caveability in block caving by effective geomechanical parameters.

Numerical modelling employing distinct element software has been used to determine the minimum required caving span. Then, relationships between the parameters affecting the minimum required caving span obtained from the numerical method have been established using multivariate regression and robust methods.

2. Artificial neural network (ANN)

ANN is a branch of artificial intelligence [22], featuring a multilayer topology with interconnected layers. A trial-and-error approach determines the number of neurons in the hidden layer. When there is a very low correlation, one of the best solutions is ANN compared to

* Corresponding author. *E-mail address:* hbakhshandeh@ut.ac.ir (H. Bakhshandeh Amnieh).

conventional alternatives, such as multivariable regression [21]. Among the different benefits of ANN modelling, function approximation and feature selection are regarded as particular capabilities.

It is required to collect an adequate number of datasets (a set of inputs and corresponding outputs) and use them for training different network architectures from which the best combination is chosen [23].

By comparing the model outputs with the measured outputs, it is possible to examine a trained network. For this purpose, four statistical indexes, including mean absolute error (MAE), determination coefficient (R^2), variance account for (VAF), and root mean square error (RMSE), should be obtained [23]. These indices can be mathematically expressed using the following formulae:

$$R^2 = 1 - \frac{\sum_{i=1}^{N}(T-T)^2}{\sum_{i=1}^{N}(T-\tilde{T})^2} \quad (1)$$

$$VAF = \left[1 - \frac{VAR(T-T)}{VAR(T)}\right] \times 100\% \quad (2)$$

$$RMSE = \sqrt{\frac{1}{N}\sum_{i=1}^{N}(T-T')^2} \quad (3)$$

$$MAE = \frac{1}{N}\sum_{i=1}^{N}|(T-T')| \quad (4)$$

Where, T, $\tilde{T}$ and T' are the measured, mean, and predicted values of T (Target), and N denotes the total number of data points.

3. Numerical Simulation

Rock mas is a mixture of intact rock and discontinuities. The properties of discontinuities affect the caveability of the rock mass. Therefore, the present research adopted the discrete element code (DEM) to simulate the jointed rock mass. For this study, the numerical model has a width of 1000 meters and a height of 350 meters (see Figure 1). The model was divided into jointed and unjointed areas. The mesh lengths in these two areas were 0.5 m and 10 m, respectively. The model was large enough to prevent the effect of boundary conditions on the caving process [1&24].

There were two parts to the model: one that was joined and one that was not. These two areas had mesh lengths of 0.5 m and 10 m, respectively [1].

using an elastic model was solved first and uniform gravitational stress was distributed within it. To further refine the models, the Mohr-Coulomb and Coulomb Slip models were applied. In other words, before creating the undercut, the model was run in the elastic state, and then the behavior of the material was changed from the elastic state to the plastic state according to the Mohr-Coulomb failure criterion, and the undercut was created. In the next steps, the material behavior model was solved according to the Mohr-Coulomb failure criterion.

Models with dip angles of 20, 70, and 90 degrees were added with persistent and close joint sets. Undercuts with dimensions of 60 and 8 m were extracted next, and a block with a height of 210 m was caved. A view of the model and its boundary condition is depicted in Figure 1.

The list of parameters and their reasonable ranges is presented in Table 1.

4. Collection of datasets

The undercut was extracted in sequential steps, and the caved area was drawn continuously and regularly. A view of displacements contours is presented in Figure 2.

A caved area was defined as any block with a displacement greater than one meter after solving the model [25]. The model was solved for this purpose. A regular and continuous extraction of caved material was simulated by removing blocks with displacements greater than one meter. Based on the numerical model, the extracted area and deformation zones are shown in Figure 3.

Various predefined and constant discontinuity models were used to increase the caving span until the caving phenomenon occurred according to a displacement criterion of 1 m. In other words, in a model with specific input data, the amount of the undercut span was changed many times until the displacement of the undercut roof reached one meter. Caving has occurred in the span where the amount of displacement reached one meter. A caved space was then created by running the model (Figure 3). Table 2 shows representative samples of 480 numerical simulation results and inputs data for 480 numerical models. Table 3 presents descriptive information about the datasets.

The results obtained from numerical modelling have already been validated by Alipenhani et al. [19] by comparing the results of physical, numerical, and empirical modelling.

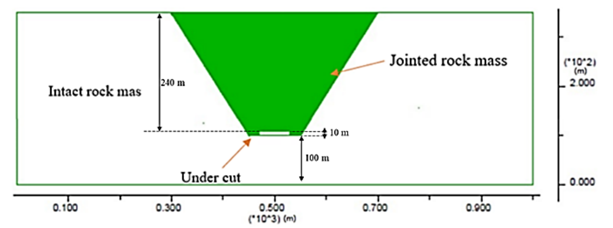

Figure 1. Numerical rock mass to model block caving.

Table 1. Input parameters of numerical modelling

Intact rock	Value	joints	Value	Parameter	Value
UCS (MPa)	130	Cohesion (MPa)	0	H (m)	500
Density (Kg/m³)	2700	Friction angle (degrees)	30	K	1
Cohesion (MPa)	4.7	Normal stiffness (GPa/m)	2	S (m)	3
Friction angle (degree)	45	Shear stiffness (GPa/m)	0.2		

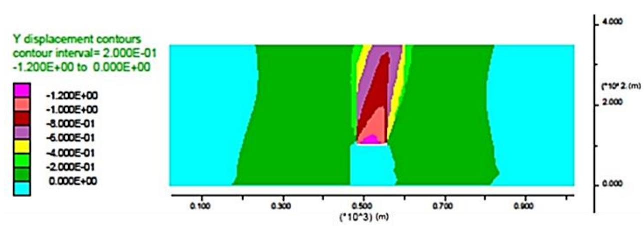

Figure 2 Displacement contours in first step of model.

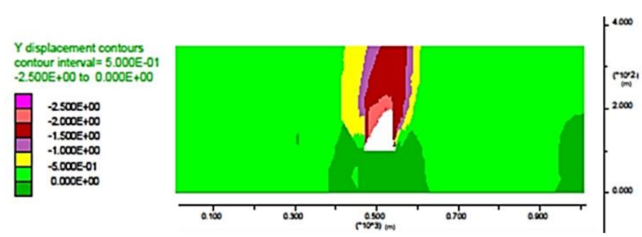

Figure 3. Displacement contours in the last step of the model.

5. Artificial Neural Networks Architecture

The present work used a backpropagation method with 480 normalized datasets to train and test groups. After pre-processing, the best model was found with a 5-28-1 architecture (Figure 4), an exponential transfer function in the output, and a logistic function in the hidden layers. The calculated R^2 of 0.981 indicates the competency of the presented ANN model (Table 4).

6. Multivariate Regression Analysis (MVR)

Using MVR, the relationship between the output and inputs was evaluated. MVR is a standard method of trend analysis in scientific functions. STATISTICA 12.0 software was used to perform regression

Table 2. Representative results of numerical simulation.

Model No.	Joint set Number (N)	Undercut Depth (H, m)	Joint Spacing (S, m)	Joint Friction angle (α, degree)	Joint Inclination (D, degree)	Minimum required caving span (MCS m)
1	3	50	1	10	70	4
2	3	50	1	30	60	8
3	3	50	1	30	70	36
4	3	100	5	35	25	50
5	3	100	5	35	45	40
6	2	200	5	35	60	22
7	2	200	5	35	70	72
8	2	400	5	35	45	38
9	2	400	5	35	60	16
10	2	400	3	23	25	12

Table 3. Variables employed for model development.

	Variables	Number	Symbol	Mean	Min	Max	Std. Dev
Input	Number of joint sets	480	N	2.50	2.0	3.0	0.50
	Joint Spacing (m)	480	S	3.0	1.0	5.0	1.63
	Angle of friction (degree)	480	α	27/6	10.0	40.0	10.45
	Joint Dip (degree)	480	D	50.0	25.0	70.0	16.97
	Depth of Undercut (m)	480	H	187/5	50.0	400.0	134.18
Output	Minimum required Caving Span (m)	480	MCS	22/72	2.0	98	19.35

Table 4. The comparison of various neural network architecture.

Number of models	Structure	Hidden function	Output function	Train dataset				Test dataset			
				R^2	MAE (m)	RMSE (m)	VAF (%)	R^2	MAE (m)	RMSE (m)	VAF (%)
1	5-28-1	Logistic	Expo.	0.983	1.92	2.56	98.16	0.981	2.13	3.00	97.84
2	5-12-1	Tanh	Sine	0.982	1.84	2.43	98.33	0.96	2.67	3.66	96.63
3	5-17-1	Logistic	Sine	0.98	1.93	2.62	32.8	0.978	2.02	3.04	97.75
4	5-28-1	Logistic	Identity	0.975	2.27	2.97	97.48	0.973	2.52	3.39	97.14
5	5-8-1	Expo.	Identity	0.962	2.85	3.7	96.06	0.95	3.42	4.46	95.18
6	5-3-1	Tanh	Logistic	0.945	3.27	4.45	94.11	0.934	3.62	5.32	92.37
7	5-10-1	Tanh	Identity	0.97	2.44	3.21	97.05	0.95	3.46	4.48	95.06
8	5-3-1	Expo.	Logistic	0.71	7.60	10.23	58.95	0.66	8.73	11.97	46.78
9	5-28-1	Sine	Expo.	0.69	8.45	10.62	49.91	0.67	9.32	11.83	40.56
10	5-8-1	Sine	Expo.	0.56	10.15	12.97	30.45	0.52	11.55	14.79	76.03

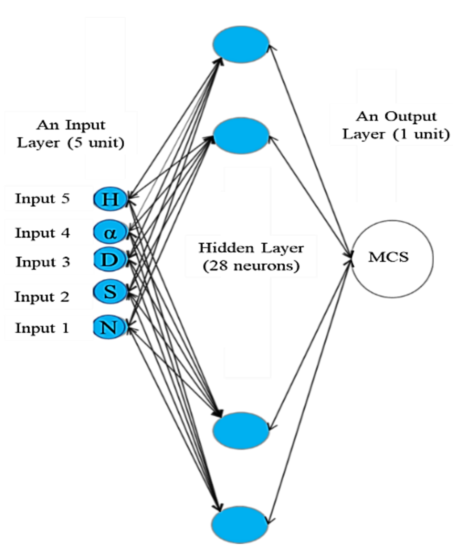

Figure 4. The optimal ANN model architecture.

analysis to develop a statistical function to predict the mean minimum required caving span (MCS) (Eq. 5). Considering this equation, joint spacing, angle of friction, and dip of joint have direct relevance to the MCS. In contrast, the number of joint sets and depth indirectly impact the magnitude of the MCS. The RMSE and determination coefficient were obtained as 11.4 and 0.61, suggesting the comparatively poorer performance of the presented MVR model compared to the ANN model.

The multivariate linear regression method was used. One of the conventional methods in multivariate analysis is the "Multiple Linear Regression" technique. Based on regression analysis, a linear relationship is established between the "Response Variable" and one or more "Explanatory Variables".

$$MCS = -6.98 - 6.13\,(\mathrm{N}) - 0.038\,(\mathrm{H}) + 5.58\,(\mathrm{S}) + 1.016(\alpha) + 15(D) \quad (5)$$

7. CART Method

A decision tree or classification tree is a part of the hierarchical technique that is widely utilized because of its capacity to cope with classification-based problems. Different parts are included in a tree's structure, such as branches, roots, nodes, and leaves. The DT is an ascending solution approach where the root is at the top of the tree. The DT approach initiates the solution by choosing a random node as the tree's potential root. Nodes denote the problem variables, and each node is classified into two branches. One of the independent variables helps in dividing the nodes. It is required to select a range during this division process by a trial-and-error approach. The performance indexes, such as RMSE, in the selected range should be minimized for each node [26].

Moreover, this approach is used for regression analysis. Since the advantages offered by the CART are more than other decision tree algorithms, researchers mostly prefer it [27]. The present study predicted the minimum required caving span by incorporating the CART approach using MATLAB software. Figure 3 indicates the decision tree developed for the MCS prediction.

As shown in Figure 5, among the five parameters studied, the angle of friction of the joint surface is the most influential parameter. This parameter converts the decision tree into two parts: one with a friction angle greater than 26.5 degrees and the other one with a friction angle less than 26.5 degrees. In rock masses where the friction angle of the joints is less than 16 degrees, the minimum required caving span will be about 5.5 meters. Otherwise, the dip of the joints and their spacing will determine the minimum required caving span. Dip and spacing are essential in rock masses with a joint friction angle greater than 26.5 degrees.

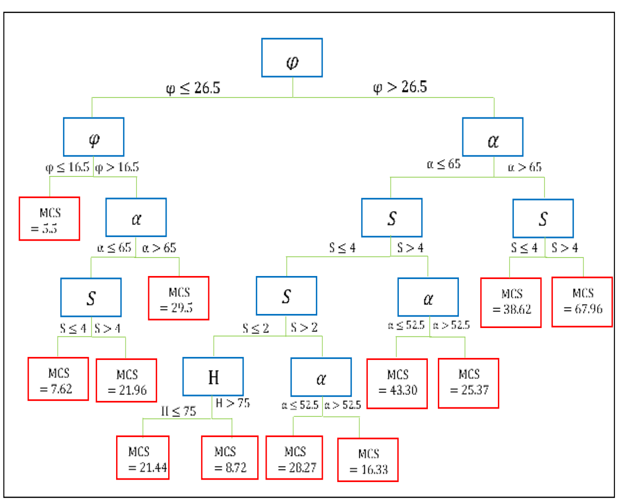

Figure 5. Developed CART model for predicting the MCS.

8. Support Vector Regression (SVR)

Support vector machines can solve both regression and classification problems. The SVM in machine learning is known for handling structural risk minimization and is extensively utilized in various research areas. The SVR is a subdivision of SVM and can be used to solve extrapolative and interpolative problems. In this SVR approach, the basis of formulation is the Vapnik–Chervonenkis (VC) theory. With a relatively low VC dimension, reasonable generalization can be reached, resulting in a low error probability [28]. Besides, a "loss function" is used in this approach for function approximation and regression estimation. The function is obtained as the difference between tube radius (ε) and predicted value. The idea of the ε-insensitive loss function is shown in Figure 6. This Figure indicates that samples situated outside the ±ε margin are regarded as non-zero slack variables, keeping them apart from calculations. The loss function amount is zero within the ε–insensitive tube. Interested readers are referred to the previous studies for more details on the SVR and SVM [21&28].

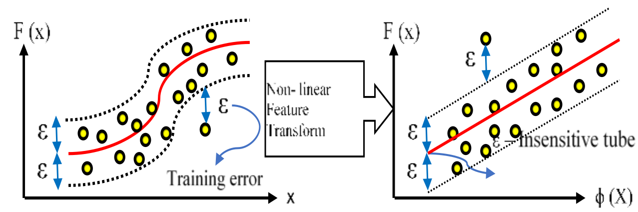

Figure 6. The graphic representation of the SVR model [28].

9. Performance assessment

The presented CART, MVR, ANN, and SVM models were evaluated with 96 (20% of the total data) new datasets in the development process. Figure 7 to 14 indicate the correlation between measured and predicted MCS for four models. The obtained values of validation indices are presented in Table 5. This table suggests that the ANN model performs better with maximum accuracy compared to the other models. In contrast, the conventional MVR has a very low efficiency compared to the other models. Additionally, as shown by the results, for problems with high nonlinearity and complexity, such as rock mass cavability, non-linear approaches with high flexibility (e.g. ANN) show higher capacities than classical linear approaches (e.g. MVR).

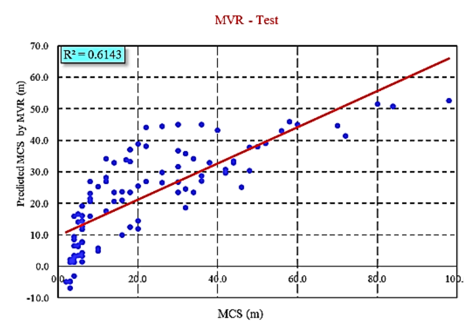

Figure 7. Scatter plot of the actual versus predicted MCS for the multivariate regression analysis method.

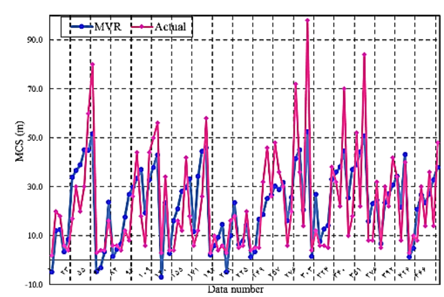

Figure 8. Comparison of measured and predicted values for the multivariate regression analysis method.

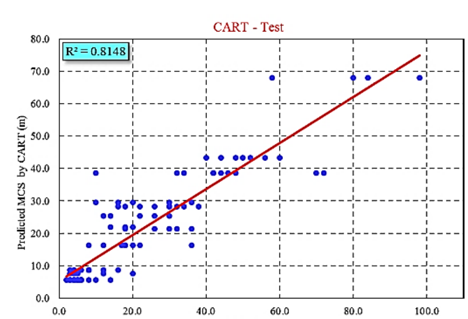

Figure 9. Scatter plot of the actual versus predicted MCS for the classification and regression tree method.

Table 5. The scores obtained in test and train data for the MVR, ANN, CART, and SVM methods.

	Train dataset				Test dataset			
Model Name	R^2	RMSE (m)	VAF (%)	MAE (m)	R^2	RMSE (m)	VAF (%)	MAE (m)
MVR	0.64	11.40	45.66	9.13	0.61	12.80	27.69	10.10
CART	0.74	9.65	67.51	6.96	0.81	9.24	67.82	6.16
SVM	0.80	8.43	74.85	6.42	0.81	9.01	75.16	7.00
ANN	0.983	2.56	98.16	1.92	0.981	3.00	97.84	2.13

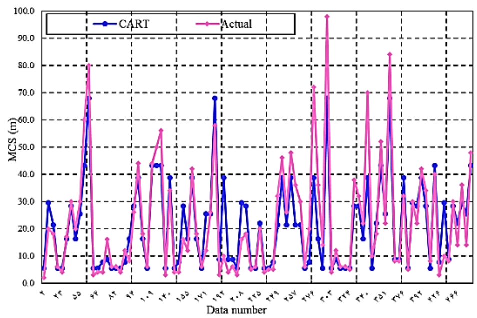

Figure 10. Comparison of measured and predicted values for the classification and regression tree method.

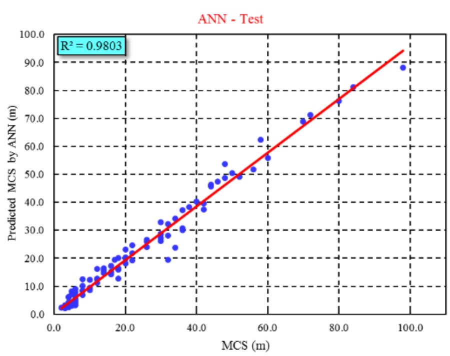

Figure 11. Scatter plot of actual versus predicted MCS by the ANN method

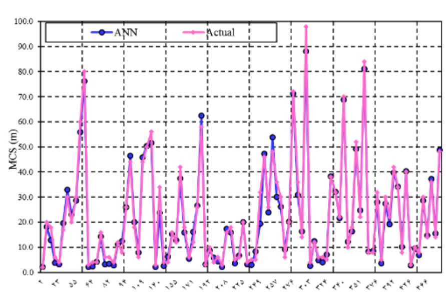

Figure 12. Comparison of measured and predicted values for the ANN method.

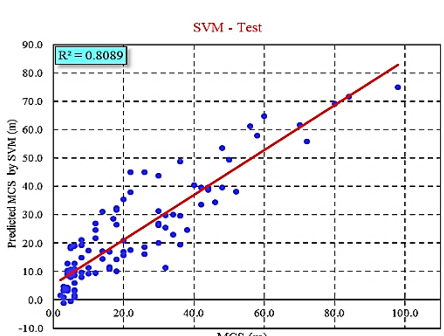

Figure 13 Scatter plot of actual versus predicted MCS for the SVMs method.

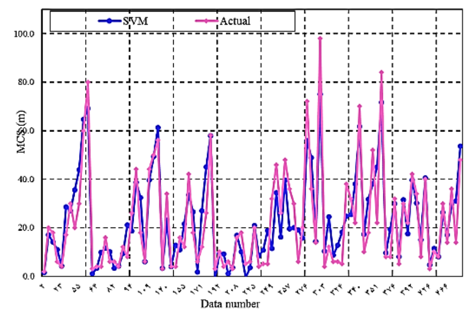

Figure 14. Comparison of measured and predicted values for the SVMs method.

10. The assessment of effect of input parameters on rock mass cavability

Generally, the sensitivity analysis (SA) is conducted to evaluate the impact of input parameters on the related outcomes. There are different sensitivity analysis methods. The relevancy factor (RF) is one of the most commonly employed approaches using the following equation [29].

$$RF = \left| \frac{\sum_{j=1}^{n}(x_{i,j}-\bar{m}_l)(y_i-\bar{m}_y)}{\sqrt{\sum_{j=1}^{n}(x_{i,j}-\bar{m}_l)^2 \sum_{i=1}^{n}(y_i-\bar{m}_y)^2}} \right| \quad (6)$$

Where:

$x_{i,j}$: the j_{th} value of the i_{th} input variable;

$\bar{m}_l$: the input variable mean;

$\bar{m}_y$: the predicted output mean.

y_i : i_{th} value of the predicted output.

Figure 15 shows that the friction angle of the joint surface had the most significant effect on the minimum required caving span. This parameter is directly related to the caving span. After the joint surface friction, joint spacing directly affects the cavability. The dip of the joints also had the most negligible effect on the minimum required caving span. The depth and number of joint sets inversely affect the cavability. In other words, the higher the number of joint sets, the greater the depth of undercut, the lower the dip angle, the shorter the joint spacing, and the lower the friction angle of the joint surface, the greater the potential for rock mass cavability.

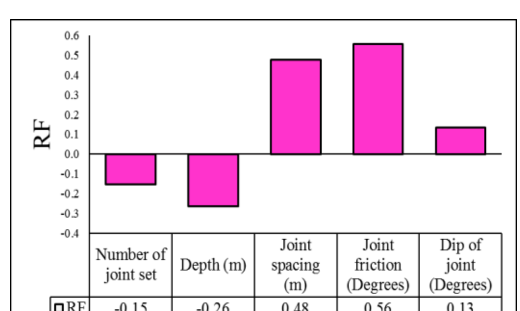

Figure 15. Effect of input parameters on the minimum required caving span.

11. Conclusions

In the present study, we implemented support vector regression, regression analysis, artificial neural network, and decision tree for investigating the impact of geomechanical parameters on the minimum required caving span in block caving mines. To this end, the database was provided from numerical modelling. Firstly, the superiority of various techniques was investigated, resulting in the approval of the neural network modelling competence. The coefficient values of MAE, RMSE, VAF, and R^2 for the ANN approach were 1.92, 2.56, 98.16% and 0.983. MVR modelling with the calculated values of 9.13, 11.40, 45.66% and 0.64 in the validation step for MAE, RMSE, VAF, and R^2 showed poor performance of this method. The results of using the network modelling application indicated that joint properties are more influential compared to the dip and number of joint sets. The angle of friction has the most significant impact and the dip of the joints has the least effect on the minimum required caving span.

Compliance with Ethical Standards

The authors declare no conflict of interest

Statements and Declarations

Funding

The authors declare that no funds, grants, or other support were received during the preparation of this manuscript.

Competing Interests

The authors have no relevant financial or non-financial interests to disclose.

Data Availability

The datasets generated during the current study are not publicly available as they have not been published yet but are available from the corresponding author on reasonable request.

REFERENCES

[1]. Alipenhani, B., Majdi, A., & Bakhshandeh Amnieh, H. (2022). Determination of caving hydraulic radius of rock mass in block caving method using numerical modeling and multivariate regression. Journal of Mining and Environment, 13(1), 217-233.

[2]. Alipenhani, B., Majdi, A., & Bakhshandeh Amnieh, H. (2022). Cavability assessment of rock mass in block caving mining method based on numerical simulation and response surface methodology. Journal of Mining and Environment, 13(2), 579-606.

[3]. Alipenhani, B., Bakhshandeh Amnieh, H., & Majdi, A. (2023). Application of Finite Element Method for Simulation of Rock Mass Caving Processes in Block Caving Method. International Journal of Engineering, 36(1), 139-151.

[4]. Alipenhani, B., Majdi, A, & Bakhshandeh Amnieh, H. (2023). Investigating mechanical and geometrical effects of joints on minimum caving span in mass caving method. International Journal of Mining and Geo-Engineering, 57(2), 223-229.

[5]. Mawdesley, C. A. (2002) Predicting rock mass cavability in block caving mines. University of Queensland.

[6]. K Suzuki Morales, FT Suorineni (2017) Using numerical modeling to represent parameters affecting cave mining. Underground Mining Technology.Australian Centre for Geomechanics, Perth, ISBN978-0-9924810-7-0.

[7]. Rafiee, R., Ataei, M., KhaloKakaie, R., Jalali, S. E., & Sereshki, F. (2016). A fuzzy rock engineering system to assess rock mass cavability in block caving mines. Neural Computing and Applications, 27, 2083-2094.

[8]. Laubscher, Cave Mining Handbook, (2000), pp. 1–138.

[9]. Mawdesley, C. A. (2002) Predicting rock mass cavability in block caving mines. University of Queensland.

[10]. Alipenhani, B., Bakhshandeh Amnieh, H., & Majdi, A. (2022b). Physical model simulation of block caving in jointed rock mass. International Journal of Mining and Geo-Engineering.

[11]. Alipenhani, B., Majdi, A., & Bakhshandeh Amnieh, H. (2024). Determination of the caving zone height using numerical and physical modeling based on the undercutting method, joint dip, and spacing, Journal of Mining and Environment.

[12]. Mohammadi, S., Ataei, M., & Kakaie, R. (2018). Assessment of the importance of parameters affecting roof strata cavability in mechanized longwall mining. Geotechnical and Geological Engineering, 36, 2667-2682.

[13]. Liu, H., Ren, F., He, R., Li, G., & Zhang, J. (2021). Application of fuzzy comprehensive assessment and rock engineering system to assess cavability in block caving mining and establishment of its regionalized model. Environmental Earth Sciences, 80, 1-13.

[14]. Rafiee, R., Ataei, M., Khalokakaie, R., Sereshki, F. (2015) Determination and Assessment of Parameters Influencing Rock Mass Cavability in Block Caving Mines Using the Probabilistic Rock Engineering System, Rock Mechanics and Rock Engineering, DOI: 10.1007/s00603-014-0614-9

[15]. Jabinpour, A., Yarahmadi Bafghi, A., Gholamnejad, J. (2018) Geostatistical modeling of rock mass cavability based on laubscher approach in Sechahoon Mine.

[16]. Majdi, A., & Beiki, M. (2010). Evolving neural network using a genetic algorithm for predicting the deformation modulus of rock masses. International Journal of Rock Mechanics and Mining Sciences, 47(2), 246-253.

[17]. Majdi, A., & Rezaei, M. (2013). Prediction of unconfined compressive strength of rock surrounding a roadway using artificial neural network. Neural Computing and Applications, 23, 381-389.

[18]. Beiki, M., Majdi, A., & Givshad, A. D. (2013). Application of genetic programming to predict the uniaxial compressive strength and elastic modulus of carbonate rocks. International Journal of Rock Mechanics and Mining Sciences, 63, 159-169.

[19]. Rezaei, M., Majdi, A., & Monjezi, M. (2014). An intelligent approach to predict unconfined compressive strength of rock surrounding access tunnels in longwall coal mining. Neural Computing and Applications, 24, 233-241.

[20]. Hasanipanah, M., Amnieh, H. B., Arab, H., & Zamzam, M. S. (2018). Feasibility of PSO–ANFIS model to estimate rock fragmentation produced by mine blasting. Neural Computing and Applications, 30, 1015-1024.

[21]. Mehrdanesh, A., Monjezi, M., Khandelwal, M., & Bayat, P. (2021). Application of various robust techniques to study and evaluate the role of effective parameters on rock fragmentation. Engineering with Computers, 1-11.

[22]. Raissi, M., Perdikaris, P., & Karniadakis, G. E. (2019). Physics-informed neural networks: A deep learning framework for solving forward and inverse problems involving nonlinear partial differential equations. Journal of Computational physics,

378, 686-707.

[23]. Li, Y., Hishamuddin, F. N. S., Mohammed, A. S., Armaghani, D. J., Ulrikh, D. V., Dehghanbanadaki, A., & Azizi, A. (2021). The effects of rock index tests on prediction of tensile strength of granitic samples: a neuro-fuzzy intelligent system. Sustainability, 13(19), 10541.

[24]. Vyazmensky, A., Elmo, D., & Stead, D. (2010). Role of rock mass fabric and faulting in the development of block caving induced surface subsidence. Rock mechanics and rock engineering, 43(5), 533-556.

[25]. Sainsbury, B. (2012). A model for cave propagation and subsidence assessment in jointed rock masses. University of South Wales.

[26]. Topal, E. (2008). Evaluation of a mining project using discounted cash flow analysis, decision tree analysis, Monte Carlo simulation and real options using an example. International Journal of Mining and Mineral Engineering, 1(1), 62-76.

[27]. Song, Y. Y., & Ying, L. U. (2015). Decision tree methods: applications for classification and prediction. Shanghai archives of psychiatry, 27(2), 130.

[28]. Wu, C. H., Ho, J. M., & Lee, D. T. (2004). Travel-time prediction with support vector regression. IEEE transactions on intelligent transportation systems, 5(4), 276-281.

[29]. Chen, G., Fu, K., Liang, Z., Sema, T., Li, C., Tontiwachwuthikul, P., & Idem, R. (2014). The genetic algorithm based back propagation neural network for MMP prediction in CO2-EOR process. Fuel, 126, 202-212